European Journal of Pharmaceutics and Biopharmaceutics 78 (2011) 346–354

Contents lists available at ScienceDirect

European Journal of Pharmaceutics and Biopharmaceutics

journal homepage: www.elsevier.com/locate/ejpb

Research paper

Drug-carrier/hydrogel scaffold for controlled growth of cells

Lan Wei [a], Jiaping Lin [a,*], Chunhua Cai [a], Zhengdong Fang [b], Weiguo Fu [b]

[a] School of Materials Science and Engineering, East China University of Science and Technology, Shanghai, China
[b] Department of Vascular Surgery, Fudan University, Shanghai, China

ARTICLE INFO

Article history:
Received 5 October 2010
Accepted in revised form 27 January 2011
Available online 18 February 2011

Keywords:
Scaffold
Drug delivery
Hydrogel
Micelle
Alginate

ABSTRACT

In this work, a novel functional drug-carrier/hydrogel scaffold was prepared to control the growth of cells for tissue engineering. The drug-carrier/hydrogel scaffold was constructed from a micelle/Ca-alginate microparticles (Alg-MPs)/poly(vinyl alcohol) (PVA) hydrogel composite. In such a system, paclitaxel (PTX) is encapsulated in the micelles formed by poly(L-glutamic acid)-*b*-poly(propylene oxide)-*b*-poly(L-glutamic acid) (GPG), while human vascular endothelial growth factor-165 ($VEGF_{165}$) is loaded in the Alg-MPs. The designed function of this scaffold is to encourage the fast growth of cells such as endothelial cells (ECs) in the early period to reduce the rejection and inhibit the growth of cells such as smooth muscle cells (SMCs) in late period to prevent the vascular intimal hyperplasia. The effect of $VEGF_{165}$ is to encourage the growth of ECs, while PTX is used to inhibit the growth of smooth muscle cells (SMCs). Structure characterizations show that the drug carriers are well dispersed in the PVA hydrogel. Independent release behaviors of the two drugs are observed. $VEGF_{165}$ shows a short-term release behavior, while PTX shows a long-term release behavior from the drug-carrier/hydrogel scaffolds. Further study shows a controllable cell growth behavior on this functional drug-carrier/hydrogel scaffold via the MTT assay.

1. Introduction

In the field of tissue engineering, functional scaffolds for controllable cell growth have attracted great attentions recently [1–15]. Hydrogel scaffolds that are incorporated with various growth factors (GFs) [3,4], peptides [5,6], or other drugs [7,8] show the ability to control cell growth [9–11], migration [12,13], and survival [14,15]. The key to control the growth of cells is the proper release behaviors of these drugs from the drug-incorporated hydrogel scaffold. Many methods have been developed to control the delivery of drugs, such as degradation-based delivery systems, affinity-based delivery systems, immobilized drug delivery systems, and electrically controlled drug delivery systems [16]. According to these methods, specific structures or functional groups of polymers should be designed to control degradation time, bind drugs, or respond to surroundings [17–21].

Comparing with fabricating complex polymers, hydrogels incorporating with nano/microparticle drug carriers show a convenient way to prepare the functional drug-loaded hydrogel scaffolds [22–25]. For example, Kim et al. have investigated an alginate hydrogel which is incorporated with dexamethasone (DEX)-loaded poly(lactic-*co*-glycolic acid) nanoparticles [22]. Such hydrogels are used for a coating of microfabricated neural probe. The results show that the in vivo impedance of the drug-loaded electrodes can be maintained at its initial level after about 2 weeks after implantation, which is attributed to the sustained release of DEX to prevent the inflammation around the implant. However, as far as we know, there are only limited reports on drug-carrier/hydrogel scaffolds so far. Researches about the drug-carrier/hydrogel scaffolds are at the initial stage. Further studies need to be done to provide deep insight into the mechanisms of these drug-carrier/hydrogel scaffolds.

For the drug vehicles, polymer micelle is one kind of extensively applied nanoparticle carriers for hydrophobic drugs [26–32]. Moreover, when introducing environmental-sensitive functional groups (pH, temperature, etc.), "smart" micelles are formed, which can be used to control drug release behaviors intelligently [28–32]. For example, Bae et al. have designed intelligent polymer micelles which are self-assembled from functional polyethylene glycol-polyamino acid (PEG-PAA) block copolymer [32]. These micelles can selectively release drugs at low pH values (pH 4–6). Hydrogel microparticles are another kind of widely adopted drug carriers especially for large molecular or water-soluble drugs [33–39]. And these hydrogel microparticles can also be environmental sensitive when they are formed by specific polymers, such as pH-sensitive polyelectrolyte [34,35] and temperature-sensitive polymers [36–39]. For instance, Jay et al. have modified the alginate microparticles to encapsulate vascular endothelial growth

* Corresponding author. Shanghai Key Laboratory of Advanced Polymeric Materials, State Key Laboratory of Bioreactor Engineering, School of Materials Science and Engineering, East China University of Science and Technology, Shanghai 200237, China. Tel.: +86 21 64253370; fax: +86 21 64251644.
E-mail addresses: jplinlab@online.sh.cn, jlin@ecust.edu.cn (J. Lin).

0939-6411/$ - see front matter © 2011 Elsevier B.V. All rights reserved.
doi:10.1016/j.ejpb.2011.01.015

factor (VEGF) [34]. These VEGF-loaded alginate microparticles achieve a controllable sustained release, which shows the potential applications as protein drug carriers. Once the hydrogel scaffolds have incorporated with these functional drug-loaded nano or microparticle carriers, the composites of drug-carrier/hydrogel scaffolds are formed. The obtained composites are expected to meet the clinical requirements for controlling the release behaviors of specific drugs [40–42].

With the fast development of clinical vascular surgery, functional vascular scaffold becomes a focus at present. The main challenge is to develop a functional scaffold for controllable cell growth. There are two key strategies for the implanted vascular scaffold: (1) inducing vascularization during the early period (about 20 days) to reduce the rejection after surgery [43,44]; (2) reducing cell growth especially the growth of smooth muscle cells (SMCs) in late period (about 3 months) to prevent the vascular intimal hyperplasia [45,46]. However, there is no example solving these two problems at one time [43–46].

In this work, for the first time, we present a novel hydrogel scaffold constructed from drug-carrier/PVA composites for controllable cell growth. To meet the clinical requirements, the human vascular endothelial growth factor-165 ($VEGF_{165}$) is encapsulated in the Ca-alginate microparticles (Alg-MPs) for a short-term release, while the paclitaxel (PTX) is encapsulated in the poly(L-glutamic acid)-*b*-poly(propylene oxide)-*b*-poly(L-glutamic acid) (PLGA-*b*-PPO-*b*-PLGA, abbreviated as GPG) micelles for a long-term release. $VEGF_{165}$ can encourage the growth of cells especially the ECs [47,48], while PTX can inhibit the growth of cells in previous studies [49,50]. The poly(vinyl alcohol) (PVA) hydrogel is used as matrix material for its good biocompatibility and physical–mechanical properties [51,52]. This drug-loaded carriers/hydrogel scaffold is intended for the potential use as vascular scaffold to encourage the growth of ECs in the early period and to inhibit the growth of SMCs in the late period after the implantation. We anticipate this scaffold can effectively reducing the rejection after surgery and prevent the vascular intimal hyperplasia. Therefore, a better treatment effect can be achieved by using this vascular scaffold to control the cell growth in clinical applications. Release behaviors of the drug carriers and drug-carrier/hydrogel scaffolds were studied as a function of pH. Then, the viabilities of endothelial cells (ECs), L929 cells, and smooth muscle cells (SMCs) on the pure PVA hydrogel (as controls) and various drug-carrier/hydrogel scaffolds were analyzed via the MTT assay. It was demonstrated that the growth of these cells can be well controlled by this functional drug-carrier/hydrogel scaffold.

2. Experimental

2.1. Materials

Tetrahydrofuran (THF), hexane, 1,4-dioxane were refluxed with sodium and distilled immediately before use. α,ω-Amino poly(propylene oxide) (NH_2-PPO-NH_2, M_w = 4000) was purchased from Sigma–Aldrich Co., Inc. Paclitaxel (PTX) was obtained from ICN Biomedicals (Costa Mesa, CA, USA). Human $VEGF_{165}$ was purchased from PeproTech Inc. (Rocky Hill, NJ, USA). Poly(vinyl alcohol) (PVA, degree of polymerization: 1750 ± 50) was purchased from Shanghai Tianlian Industry of Fine Chemicals Co., Ltd. Alginate was obtained from Sinopharm Chemical Reagent Co., Ltd. The ECs, L929 cells and SMCs were obtained from Shanghai Institute of Biochemistry and Cell Biology, Chinese Academy of Sciences. Cellulose membrane dialysis bag (3500 molecular weight cut-off) was provided by Serva Electrophoresis GmbH. All other reagents are of analytical grade and used without further purification.

2.2. Synthesis and characterization of triblock copolymer

The poly(γ-benzyl-L-glutamate)-*b*-poly(propylene oxide)-*b*-poly(γ-benzyl-L-glutamate) (PBLG-*b*-PPO-*b*-PBLG) triblock copolymer was synthesized by ring-opening polymerization of γ-benzyl-L-glutamate-N-carboxyanhydride (BLG-NCA) initiated by terminal amino groups of NH_2-PPO-NH_2. The PLGA-*b*-PPO-*b*-PLGA triblock copolymer was prepared by hydrolyzation of PBLG-*b*-PPO-*b*-PBLG with potassium hydroxide (KOH). Molecular weight of the PLGA-*b*-PPO-*b*-PLGA triblock copolymer was estimated by ^{1}H NMR measurements (Avance 550, Bruker). The total molecular weight of the triblock copolymer was calculated as 10,900 based on the known degree of polymerization (DP) of PPO (DP = 69, M_w = 4000). All the details were available in our previous reports [53–55].

2.3. Preparation of Ca-alginate microparticles

Ca-alginate microparticles were prepared using a double emulsion method. Ten milliliters Na-alginate solution (15 mg/mL), 50 mL paraffin oil, and 0.6 mL Span 85 were mixed together. The mixture was stirred at 3000 rpm for 15 min to form the water-in-oil (w/o) emulsion. The Na-alginate w/o emulsion was then added into 20 mL 10 wt.% $CaCl_2$ solution containing 0.2 mL Tween 80 at a rate of 1 drop per second to form the water-in-oil-in-water (w/o/w) double emulsion. The Na-alginate droplets rapidly gelled in the w/o/w emulsion, and the suspension was stirred for 1 h for further gelation. The obtained Ca-alginate microparticles were collected by centrifugation, washed three times by ethanol and water, and lyophilized before use.

2.4. Preparation of the drug-carrier/hydrogel scaffolds

The loading amount of PTX in GPG micelles (micelle concentration is 0.3 mg/mL) as a function of initial PTX amount has been studied first. It shows that the loading amount of PTX is increased with increasing initial PTX amount. However, the loading amount increases indistinctively when the initial PTX amount is over 0.25 mg/mL. Therefore, the PTX-loaded micelle solution was prepared as follows: 3 mg PLGA-*b*-PPO-*b*-PLGA was first dissolved in 10 mL 0.1 M KOH aqueous solution. Then, 0.5 mL PTX ethanol solution (5 mg/mL) was added with vigorous stirring. The mixed solution was dialyzed against distilled water for 3 days at 20 °C to form the PTX-loaded GPG micelle. The average diameters of GPG micelles are 104 nm and 141 nm before and after encapsulating the PTX by the DLS spectrometer (ALV/CGS-5022).

The $VEGF_{165}$-loaded Ca-alginate microparticles (Alg-MPs) were prepared as follows: 20 μL $VEGF_{165}$ PBS solution (0.1 μg/μL) was mixed with 30 mg lyophilized Ca-alginate microparticles. Then, the samples were placed at 4 °C until $VEGF_{165}$ was fully absorbed. After that, the $VEGF_{165}$-loaded Alg-MPs were washed with PBS solution to remove the free $VEGF_{165}$. No diameter change of Alg-MPs is observed after encapsulating the $VEGF_{165}$.

The PTX-loaded GPG micelle/$VEGF_{165}$-loaded Ca-alginate microparticle/PVA hydrogel (PTX-GPG/$VEGF_{165}$-Alg/PVA) scaffold was obtained by mixing the pre-made PTX-loaded GPG micelles, $VEGF_{165}$-loaded Alg-MPs and PVA solution together, followed by a freezing–thawing cycle (freezing at −20 °C for 24 h and thawing at room temperature for 3 h) in a 24-well plate. The mixture was comprised of 4.0 wt.% PVA, 0.15 wt.% PTX-loaded GPG, and 0.3 wt.% $VEGF_{165}$-loaded Alg-MPs. Therefore, the concentrations of $VEGF_{165}$ and PTX are chosen to be about 0.2 μg/mL and 0.4 mg/mL in the mixture, respectively, according to the literatures [56,57]. The drug-carrier/hydrogel scaffolds with various Alg-MPs contents were prepared by the same method. All the drug-carrier/hydrogel scaffolds were washed with distilled water to remove the free GPG micelles and Alg-MPs. And the distilled water

was collected, sonicated, and the concentration of PTX and $VEGF_{165}$ were tested by ultraviolet–visible spectrometer and ELISA, respectively. Details of the drug concentration tests were provided in Section 2.5.

2.5. Loading efficiency

The amount of PTX encapsulated in the GPG micelles was analyzed by an ultraviolet–visible spectrometer (UV/vis, Unico UV2102). Eight milliliters methanol was introduced into 2 mL PTX-loaded micelle solution, and the mixture was sonicated for 30 min. The micelles were broken up, and the PTX was dissolved in the solution. The characteristic absorbance of PTX at 227 nm was recorded and compared with a standard curve generated from a methanol/H_2O (v/v = 4/1) mixture with PTX concentrations varying from 0 to 100 μg/mL.

The loading efficiency of $VEGF_{165}$ in Alg-MPs was determined as follows: In the preparation process, the drug-loaded particles were washed by PBS solution after $VEGF_{165}$ was fully absorbed into Alg-MPs to remove free $VEGF_{165}$. Then, the PBS wash-solution was collected, and the concentration of $VEGF_{165}$ was measured by ELISA. ELISA was performed according to the procedure of the kit (R&D systems) [12]. The $VEGF_{165}$ loading amount was calculated by subtracting the free drug amount from the total drug amount.

2.6. Characterization of the drug-carrier/PVA hydrogel scaffold

Morphologies of the drug-carrier/PVA hydrogel scaffold were observed by transmission electron microscope (TEM, JEM 1200-EXII, operated at 120 kV) and scanning electron microscope (SEM, JSM 6460, JEOL, operated at 20 kV). The samples for TEM observations were prepared by placing drops of the PTX-GPG/$VEGF_{165}$-Alg/PVA mixture on a carbon film-coated copper grid and then followed by a freezing–thawing cycle. These samples were pre-stained in solution by phosphotungstic acid aqueous solution (0.5 wt.%). All the samples were then dried at room temperature.

Size distribution of alginate hydrogel particles were analyzed by a laser particle analyzer (LPA, BT-9300H, Dandong Bettersize instruments Ltd.). Alginate particles were suspended in the PBS solutions with various pH values for 3 days before test.

The average pore size of the drug-carrier/PVA hydrogel scaffolds were determined by the different scanning calorimeter (DSC, Perkin-Elmer, Diamond DS) measurements. This method is based on the dependence of the freezing point on the size of microcrystals [58,59]. In this work, the hydrogel is saturated by water, and the average pore size of the hydrogel can be calculated by the solidification temperature of the system. Experiments were performed as follows: sample were weighted and put in a sealed aluminum pan, and one drop of water was added to maintain the samples in an excess of solvent. Then, the samples was first cooled to −40 °C and then heated up and kept isothermally at −0.3 °C for 10 min. Thereafter, the pan was cooled down to −40 °C at a rate of 1 °C/min. The pore size of hydrogel can be calculated by the following equation [58,59]:

$$R_p\ (\mathrm{nm}) = -\frac{64.67}{\Delta T} + 0.57 \quad (1)$$

where R_p is the pore radius at temperature T, $\Delta T = T - T_0$ and T_0 is the normal triple point temperature.

2.7. In vitro drug release study

A fixed volume of $VEGF_{165}$-loaded Ca-alginate microparticle suspension and PTX-loaded GPG micelle solution were suspended in a dialysis bag, respectively, and placed into 10 mL buffer solution with various pH values. And the PTX-GPG/$VEGF_{165}$-Alg/PVA hydrogel scaffolds were directly immersed in 10 mL buffer solutions. Samples were then laid in a shaking bath at 90 rpm, with constant temperature of 37 °C. The buffer solution was replaced periodically. UV/vis absorbance was recorded at 227 nm, and the concentrations of PTX in buffer solutions were determined according to the standard curve of PTX at corresponding buffer solutions. The concentration of $VEGF_{165}$ was determined by ELISA. And then the release amount of each drug can be calculated. Three replicates were measured, and the results were averaged with standard deviation.

2.8. Cell culture

The 96-well plates were pre-coated with PVA (as controls), PTX-GPG/PVA, $VEGF_{165}$-Alg/PVA, and PTX-GPG/$VEGF_{165}$-Alg/PVA hydrogels, respectively. The endothelial cells (ECs) were cultivated onto the pre-coated 96-well plates with the concentration of 5×10^3 cells/well in Medium 199 (M199) containing 10% fetal bovine serum (FBS), 25 ng/mL basic fibroblast growth factor (bFGF), 100 μg/mL penicillin, and 100 μg/mL streptomycin. The L929 cells were cultivated with the concentration of 1×10^3 cells/well in Dulbecco's Modified Eagle Medium (DMEM) containing 10% fetal bovine serum (FBS), 100 μg/mL penicillin, and 100 μg/mL streptomycin. And the smooth muscle cells (SMCs) were cultivated with the concentration of 5×10^3 cells/well in DMEM. Cells were all cultivated with the condition of 37 °C and 5% CO_2.

2.9. Viability analysis

The viability of endothelial cells (ECs), L929 cells, and smooth muscle cells (SMCs) was studied by the tetrazolium salt (MTT) assay at regular time intervals. The MTT solution (100 μL, 0.5 mg/mL in PBS solution) was added to each well for 4 h, at 37 °C. Then, MTT was aspirated, and 100 μL DMSO was added. Subsequently, the absorbance at 540 nm was measured using a UV/vis spectrometer. MTT assay were repeated in three separate experiments. The results are represented as a percentage of absorbance relative to control cells (cells on PVA hydrogel).

2.10. Statistical analysis

Statistical analysis of the difference between each group was tested by one-way ANOVA (SPSS software). Results were considered significant differences when $P < 0.05$.

3. Results and discussion

This paper consists of three sections: in the first section, we characterized the structures of drug-carrier/PVA hydrogel scaffolds. In the second section, in vitro release behaviors of $VEGF_{165}$ from Alg-MPs, PTX from GPG micelles, and the two drugs from the PTX-GPG/$VEGF_{165}$-Alg/PVA hydrogel scaffolds were investigated as a function of pH. In the last section, the viabilities of endothelial cells (ECs), L929 cells, and smooth muscle cells (SMCs) on the pure PVA hydrogel, PTX-GPG/PVA, $VEGF_{165}$-Alg/PVA, and the PTX-GPG/$VEGF_{165}$-Alg/PVA hydrogel scaffolds were analyzed by the MTT assay.

3.1. Characterization of the drug-carrier/PVA hydrogel scaffold

We first studied the morphologies of the drug-carrier/PVA hydrogel scaffold. Images of the drug-carrier/PVA hydrogel scaffolds from TEM and SEM observations are shown in Fig. 1a and b, respectively. The distribution of the PTX-loaded GPG micelles in

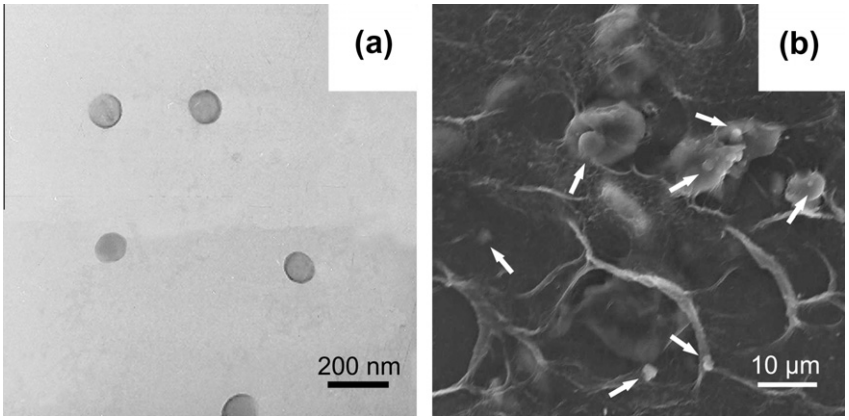

Fig. 1. (a) TEM photograph of PTX-loaded GPG micelles in PVA hydrogel scaffold and (b) SEM photograph of $VEGF_{165}$-loaded Alg-MPs in PVA hydrogel scaffold.

PVA hydrogel was observed by TEM. A representative image is presented in Fig. 1a. As can be seen, spherical micelles with diameter of about 110 nm are well dispersed in the hydrogel matrix. Fig. 1b shows the SEM image of the Alg-MPs in drug-carrier/PVA hydrogel scaffold. These Alg-MPs with diameter about 4–6 μm are embedded in the hydrogel network (marked by the white arrow), and the distribution is fine.

We also examined the pH sensitivity of Ca-alginate microparticles by analyzing the particle size distribution at various pH values. The initial average diameter (MD) of Alg-MPs is 61.20 μm, and these Alg-MPs can be fully restored after lyophilization. Table 1 shows the average particle size of alginate microparticles (Alg-MPs) as a function of pH values. Compared with the diameters of dried Alg-MPs (see Fig. 1b), the average diameter of these swelled Alg-MPs shows more than 10-fold increase (see Table 1). Moreover, the particle size of Alg-MPs increases from the average medium diameter (MD) = 52.36 μm at pH = 6.2 to MD = 77.49 μm at pH = 8.4, indicating a pH-sensitive swelling behavior of Alg-MPs. Alginate is a typical anionic polymer which contains acidic groups on the molecular chain. These acidic groups can be deprotonated in high pH value conditions, leading to a swelling behavior of alginate hydrogel via the electrostatic repulsion [60–64]. Therefore, the diameters of Alg-MPs increase with increasing pH value.

3.2. In vitro drug release study

The release behaviors of $VEGF_{165}$ from Alg-MPs and PTX from GPG micelles were first studied. The obtained loading contents and efficiencies of $VEGF_{165}$ and PTX are listed in Table 2. The $VEGF_{165}$-loaded Alg-MPs and the PTX-loaded GPG micelles show high loading efficiencies, which indicates these carriers are suitable to deliver the corresponding drugs.

Release profiles of $VEGF_{165}$ from the Alg-MPs at 37 °C as a function of pH are shown in Fig. 2a. $VEGF_{165}$ is released completely within 2 days in all the three pH conditions. The release behavior of $VEGF_{165}$ is pH sensitive. The release rate is increased with increasing pH value. The pH-controlled release of $VEGF_{165}$ is caused by the pH sensitive of Alg-MPs. Alg-MPs swell in high pH condition (see Table 1). The pore size of Ca-alginate network is enlarged in the swelling of Alg-MPs, leading to a broadened release tunnel to accelerate the release of $VEGF_{165}$ [52–54]. In addition, the release rate of $VEGF_{165}$ from Alg-MPs can be modified by

Table 1
Diameters of Alg-MPs in various pH buffer solutions (pH = 6.2, 7.3, and 8.2).

	pH = 6.2	pH = 7.3	pH = 8.2
Medium diameter (μm)	52.36	62.76	77.49
Volume mean diameter (μm)	54.57	64.73	78.27
Surface mean diameter (μm)	39.26	56.59	61.86

Table 2
Drug-loading content and efficiency of GPG micelles and Alg-MPs.

	Loading content[a] (wt.%)	Loading efficiency[b] (%)
PTX-load GPG micelles	28.6	48.3
$VEGF_{165}$-load alginate MPs	–[c]	96.7

[a] The loading content was defined as the ratio of the weight of the loading drug to the weight of drug and copolymers in drug-loaded micelle solution.
[b] The loading efficiency was defined as the ratio of the weight of loaded drug to the initially added drug.
[c] The loading content of $VEGF_{165}$-alginate MP is less than 0.1‰ because of the low concentration of $VEGF_{165}$ solution.

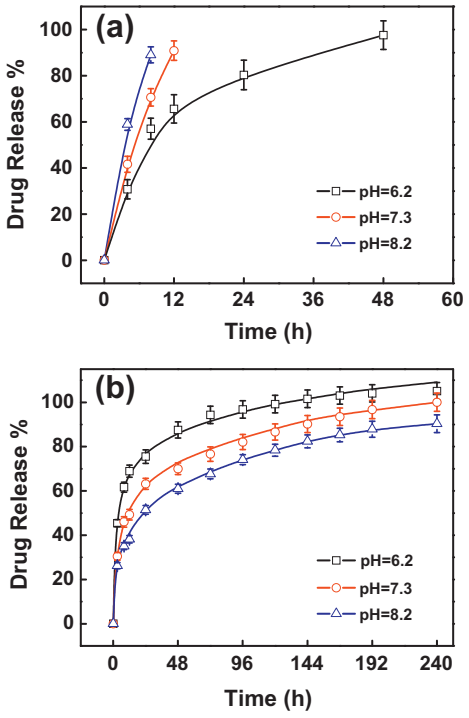

Fig. 2. (a) Release profiles of $VEGF_{165}$ from Alg-MPs at 37 °C as a function of pH and (b) release profiles of PTX from GPG micelles at 37 °C as a function of pH. (For interpretation of the references to color in this figure legend, the reader is referred to the web version of this article.)

changing the cross-linking time of Alg-MPs carriers (see Fig. S1a in Supplementary material). The drug release rate can be reduced by prolonging the cross-linking time of Alg-MPs carriers. Fig. 2b shows the release profiles of PTX from GPG micelles. Compared to $VEGF_{165}$, PTX shows a long-term release behavior which lasts for over 7 days especially in high pH condition. The release behavior of PTX also shows pH dependence. The fastest release rate of PTX from GPG micelles appears in the lowest pH condition (pH = 6.2). Nearly 100% amount of the loaded PTX is released in 144 h. As the pH value is increased, the release rate of PTX slows down, leading to a much longer release time of PTX in higher pH conditions. The pH-controlled release behavior of PTX is due to the pH sensitivity of the PLGA segments which form the micelle corona. At low pH value, the PLGA segments transform from coil to α-helix conformation and shrink [65–68]. This generates a stress on the core of micelle at low pH value, which gives rise to a core distortion. PTX leaks from the micelles. As a result, PTX shows an accelerated release at lower pH value [54,55]. It should be note that the saturation solubility of PTX shows negligible pH dependence according to our test (ca. 15.3 μg/mL in pH 6.0–8.2). The pH-dependant release behavior of PTX could be entirely caused by GPG micelles. Besides, the release period of PTX from GPG micelles can be extended by cross-linking the PLGA shells of the micelles (see Fig. S1b in Supplementary material).

We then examined the drug releasing behavior of the PTX-GPG/$VEGF_{165}$-Alg/PVA hydrogel scaffold. Fig. 3 shows the release profiles of the PTX-GPG/$VEGF_{165}$-Alg/PVA hydrogel scaffolds at 37 °C as a function of pH. $VEGF_{165}$ releases fast to about 95% in the first 3 days, while PTX shows a sustained release which lasts for more than 10 days. Both $VEGF_{165}$ and PTX show a pH-sensitive releasing as can be seen from Fig. 3. These results indicate that the release behaviors of drugs in the PVA hydrogel scaffold are mainly controlled by their respective carriers (comparing Fig. 3 with Fig. 2a and b). Such drug-carrier/hydrogel scaffold shows an independent controllable drug release behaviors associated with the incorporated functional carriers. This function is consistent with the clinical requirements for an implant vascular scaffold.

Interestingly, our study shows that the existence of Ca-alginate microparticles has a marked effect of reducing the release rate of PTX. We investigated the PTX-GPG/$VEGF_{165}$/PVA system ($VEGF_{165}$ is directly dispersed in PVA hydrogel) in comparison with the PTX-GPG/$VEGF_{165}$-Alg/PVA hydrogel scaffold. The release profiles of the two drugs from both PTX-GPG/$VEGF_{165}$/PVA and PTX-GPG/$VEGF_{165}$-Alg/PVA hydrogel scaffold are shown in Fig. 4. The measurements were carried at 37 °C and pH = 7.3. The results show that the $VEGF_{165}$ has a short-term release behavior in both systems. However, the release rate of PTX from PTX-GPG/$VEGF_{165}$-Alg/PVA hydrogel scaffold is much slower than that from

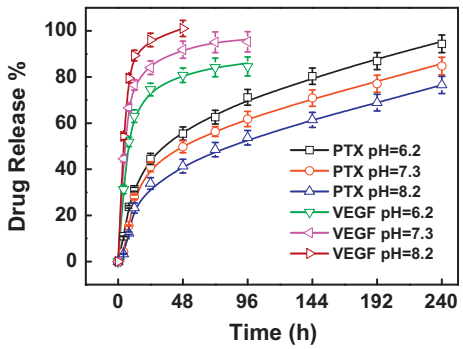

Fig. 3. Release profiles of PTX and $VEGF_{165}$ from PTX-GPG/$VEGF_{165}$-Alg/PVA hydrogel scaffold at 37 °C as a function of pH. (For interpretation of the references to color in this figure legend, the reader is referred to the web version of this article.)

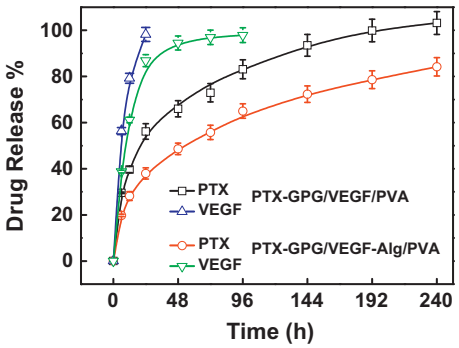

Fig. 4. Release profiles of PTX and $VEGF_{165}$ from PTX-GPG/$VEGF_{165}$/PVA hydrogel scaffold and PTX-GPG/$VEGF_{165}$-Alg/PVA hydrogel scaffold, T = 37 °C, pH = 7.3. (For interpretation of the references to color in this figure legend, the reader is referred to the web version of this article.)

PTX-GPG/$VEGF_{165}$/PVA hydrogel scaffold. The only difference is the existence of the Ca-alginate microparticles in the rate reduced system. It should be emphasized that the difference in the release behaviors of $VEGF_{165}$ between the two systems is relative small. This can be attributed to the fast release rates of the $VEGF_{165}$.

To further unveil the mechanism behind the release behavior, influence of existence of Alg-MPs in the PTX-GPG/PVA hydrogel systems were investigated. Fig. 5a shows the release profiles of PTX from the PTX-GPG/PVA, PTX-GPG/PVA/alginate (the alginate is in form of dispersed state), and the PTX-GPG/PVA/Alg-MPs systems with various Alg-MPs contents at 37 °C and pH = 7.3. The release rate of PTX changes very little within the addition of alginate polymer; however, the release rate of PTX decreases significantly when adding Alg-MPs in the same content (both are

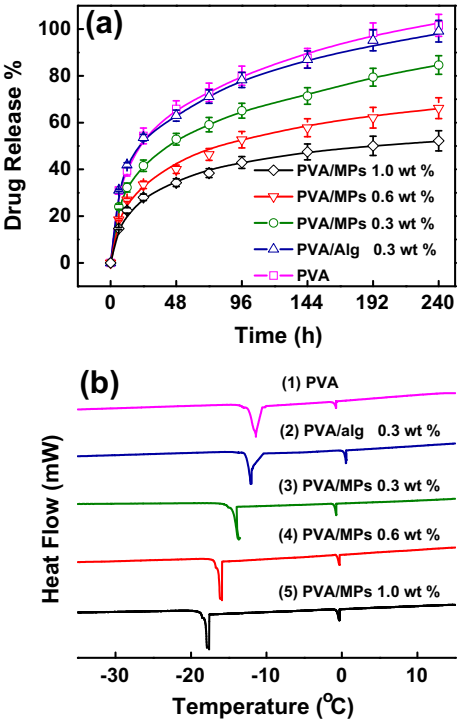

Fig. 5. (a) Release profiles of PTX (encapsulated in GPG micelle) from PVA hydrogel, PVA/alginate, and PVA/Alg-MPs composites with various Alg-MPs contents, T = 37 °C, pH = 7.3 and (b) the solidification thermogram of water contained in PTX-PVA, PTX-PVA/alginate, and PTX-PVA/Alg-MPs composite hydrogel systems (cooling rate = 1 K/min). (For interpretation of the references to color in this figure legend, the reader is referred to the web version of this article.)

0.3 wt.%). Moreover, the release rate of PTX is further decreased with the increase of Alg-MPs content.

In order to explain this Alg-MPs-induced drug release rate decrease, we have tested the average pore size of these composite systems by the DSC method [58,59]. The solidification thermogram recorded for these composite hydrogels is given in Fig. 5b. The temperature peaks of the DSC profiles show the solidification temperature of water inside these composite hydrogels, respectively. The water solidification temperatures (peak temperature) of PTX-GPG/PVA and PTX-GPG/PVA/alginate hydrogel are very close to each other and are both higher than that of the PTX-GPG/PVA/Alg-MPs systems. Moreover, the peak temperature of the PTX-GPG/PVA/Alg-MPs system is decreased with increasing Alg-MPs content, indicating a pore size decrease with increasing Alg-MPs content. The solidification peaks at about 0 °C were attributed to the freezing of free water outside the hydrogel. The peak temperature and average pore diameters (calculated from Eq. (1)) of these composite systems are listed in Table 3. The pore size of the Alg-MPs/PVA composite systems decreases with increasing Alg-MPs content. However, the average pore diameter changes little in PVA/alginate composites compared with pure PVA hydrogel (see Table 3).

The different release behavior of PTX (encapsulated in GPG micelle) from PVA and Alg-MPs/PVA system can be explained as follows: after the PTX releasing from the GPG micelles, it begins to diffuse through the pores of the hydrogel network. The drug diffusion rate is strongly influenced by the pore size of the hydrogel network, which can be decreased by reducing the pore size [69,70]. When the Alg-MPs was added into the system, they can partially or completely block the surrounding hydrogel pores, because the volumes of Alg-MPs are much larger than the PVA pore size (see Table 1 and Table 3). Subsequently, the average pore size of the hydrogel system is reduced (see Table 3), leading to a much narrowing passage for PTX to release. As a result, the release rate of PTX is decreased when adding Alg-MPs into the PTX-GPG/PVA system. Drug release controlled by the existence of the microparticles is an interesting finding of present work. It provides a new way to manipulate the drug release behavior outside the carriers. Such a finding can greatly simplify the preparation of controlled release systems. In addition, this system can be flexibly modified by simply adjusting these Alg-MPs to meet various clinical requirements.

3.3. MTT assay

With the knowledge of the controllable release behaviors of the drug-carrier/hydrogel scaffolds, the viabilities of endothelial cells (ECs), L929 cells, and smooth muscle cells (SMCs) on the drug-carrier/PVA hydrogel scaffold were studied by the MTT assay. Cells were cultured on various drug-carrier/PVA hydrogel scaffolds (pure PVA, PTX-GPG/PVA, $VEGF_{165}$-Alg/PVA, and PTX-GPG/$VEGF_{165}$-Alg/PVA) in about 10 days to observe the cell growth behaviors. The ultimate goal for the PTX-GPG/$VEGF_{165}$-Alg/PVA hydrogel scaffold is to encourage fast growth of cells especially ECs in the early period to reduce the rejection and inhibit the growth of cells especially smooth muscle cells (SMCs) in late period to prevent the vascular intimal hyperplasia.

The optical density (OD) value of cells on PVA hydrogel was taken as controls. Cells growing in the control wells were taken as 100% viability, and further comparisons were based on that reference level. The viabilities (% of control) were then calculated as follows:

$$\text{Viability (\% control)} = \left(\frac{OD_{sample}}{OD_{control}}\right) \times 100 \quad (2)$$

where OD_{sample} is the OD value of cells on drug-carrier/hydrogel scaffold (PTX-GPG/PVA, $VEGF_{165}$-Alg/PVA, and PTX-GPG/$VEGF_{165}$-Alg/PVA, respectively) and $OD_{control}$ is the OD value of cells on PVA hydrogel at various culture times.

Viabilities of ECs on various drug-carrier/hydrogel scaffolds are shown in Fig. 6a. ECs cultivated on $VEGF_{165}$-Alg/PVA and PTX-GPG/$VEGF_{165}$-Alg/PVA scaffold show the higher viabilities, while ECs on PTX-GPG/PVA scaffold shows the lower viability during the first 3 days. This can be explained by the fact that the fast released $VEGF_{165}$ from $VEGF_{165}$-Alg/PVA or PTX-GPG/$VEGF_{165}$-Alg/PVA hydrogel scaffold can encourage the growth of ECs in the early period. From Fig. 6a, one can see that the viability of ECs in the early

Table 3
Average pore diameters of the PTX-GPG/PVA, PTX-GPG/PVA/alginate (in the form of dispersed state), and PTX-GPG/PVA/Alg-MPs hydrogel scaffolds with various Alg-MPs contents.

Alg-MPs content	0 wt.%	0.3 wt.% (dispersed)	0.3 wt.%	0.6 wt.%	1.0 wt.%
Peak temperature (°C)	−11.33	−11.87	−13.67	−15.81	−17.50
Average pore diameter (nm)	12.56	12.04	10.6	9.32	8.52

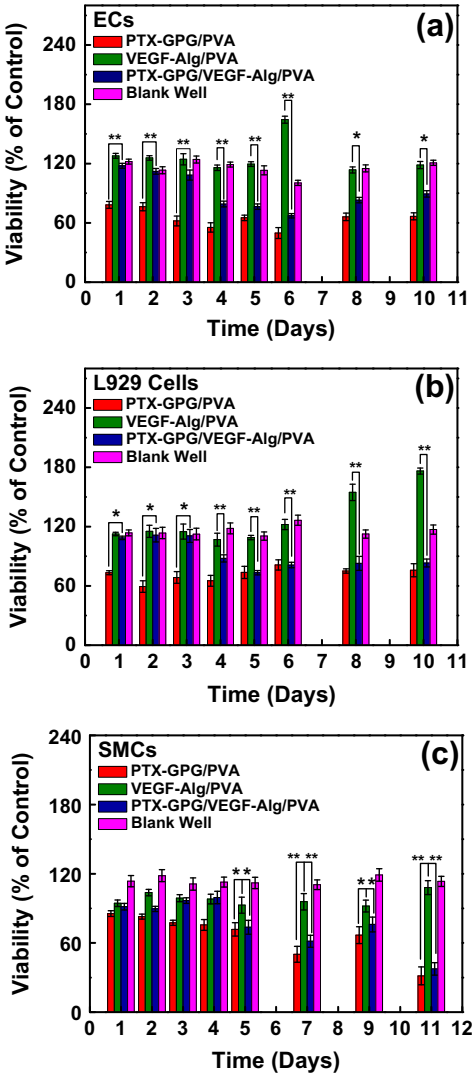

Fig. 6. MTT assay of cell viabilities of ECs (a), L929 cells (b), and SMCs (c). ($^{*}p < 0.01$, $^{**}p < 0.0001$). (For interpretation of the references to color in this figure legend, the reader is referred to the web version of this article.)

period on the PTX-GPG/$VEGF_{165}$-Alg/PVA scaffold is at the same level of that on $VEGF_{165}$-Alg/PVA scaffold ($P > 0.05$), but much higher than that on PTX-GPG/PVA scaffold ($P < 0.0001$). This indicates that the growth of ECs on the PTX-GPG/$VEGF_{165}$-Alg/PVA scaffold is mainly controlled by the fast release of $VEGF_{165}$ from the scaffold in the early time. The viability of ECs on PTX-GPG/$VEGF_{165}$-Alg/PVA scaffold is then sharply decreased during the next 7 days as can be seen from Fig. 6a. Contrary to the results in the early period, the viability of ECs on PTX-GPG/$VEGF_{165}$-Alg/PVA scaffold is similar to that on PTX-GPG/PVA scaffold ($P > 0.05$) and much lower than that on $VEGF_{165}$-Alg/PVA scaffold ($P < 0.01$). This reveals that the growth of ECs on the PTX-GPG/$VEGF_{165}$-Alg/PVA hydrogel system can be inhibited by the sustained and long-term release of PTX from the scaffold in late period. The viabilities of ECs on the blank well (without any gel) are lower than 120% during the test period, which indicates that the PVA hydrogel is biocompatible for ECs.

Similar results were observed in the growth of L929 cells on various drug-carrier/hydrogel scaffolds. Shown in Fig. 6b are the viabilities of L929 cells on PTX-GPG/PVA, $VEGF_{165}$-Alg/PVA, and PTX-GPG/$VEGF_{165}$-Alg/PVA hydrogel scaffolds. L929 cells show an encouraged growth on $VEGF_{165}$-Alg/PVA scaffold and an inhibited growth on PTX-GPG/PVA during the whole period. And the growth of L929 cells on PTX-GPG/$VEGF_{165}$-Alg/PVA hydrogel scaffold is encouraged in the first 3 days ($P > 0.05$, for L929 cells on PTX-GPG/$VEGF_{165}$-Alg/PVA vs. on $VEGF_{165}$-Alg/PVA) and inhibited in the late period ($P > 0.05$, for L929 cells on PTX-GPG/$VEGF_{165}$-Alg/PVA vs. PTX-GPG/PVA). L929 cells on blank wells show the viabilities around 115%, indicating the biocompatibility of PVA hydrogel for L929 cells.

Fig. 6c shows the viabilities of smooth muscle cells (SMCs) on PTX-GPG/PVA, $VEGF_{165}$-Alg/PVA, and PTX-GPG/$VEGF_{165}$-Alg/PVA scaffolds, respectively. No significant difference between the $VEGF_{165}$-Alg/PVA scaffold and PVA hydrogel (as controls) is observed in the whole period, because the $VEGF_{165}$ has no effects on the growth of SMCs [71,72]. The viability of SMCs on PTX-GPG/PVA scaffold shows a slight decrease in the first 4 days and a shape decrease in late period. Comparing with the $VEGF_{165}$-Alg/PVA and PTX-GPG/PVA scaffolds, the PTX-GPG/$VEGF_{165}$-Alg/PVA scaffold shows a delayed inhibition effect on SMCs growth. The inhibition effect from the PTX-GPG/$VEGF_{165}$-Alg/PVA scaffold becomes marked after 7 days. This is caused by the delayed release of PTX from PTX-GPG/$VEGF_{165}$-Alg/PVA scaffold.(see Fig. 4 and Fig. 5a). And the viabilities of SMCs on the blank well are kept to 110–118%, which shows the biocompatibility of PVA hydrogel for SMCs.

Morphologies of ECs, L929 cells, and SMCs were observed by optical microscopy. Fig. 7 shows the morphology photographs of ECs, L929 cells, and SMCs cultivated on the PTX-GPG/$VEGF_{165}$-Alg/PVA scaffold at day 2. Cells are all cultivated with the concentration of 5×10^4 cells/well. ECs appear as multiple morphologies such as sphere and fusiform shape; L929 cells take the form of spindle shape; and the SMCs present a long shuttle-shape on the hydrogel scaffolds. All the three kinds of cells show typical morphologies, respectively, on the hydrogel scaffold, indicating a good biocompatibility and cell adhesion of the PTX-GPG/$VEGF_{165}$-Alg/PVA scaffold. In addition, the growth of cocultured ECs and SMCs is also observed. ECs grow well at day 2, and both ECs and SMCs show their typical morphologies on the composite scaffold. For detailed information, see Fig. S2 in Supplementary material.

The MTT assay and microscopy observation result demonstrates that the controllable cell growth is successfully achieved on this drug-carrier/hydrogel scaffold. The growth of ECs and L929 cells are encouraged in early period due to the quick release of $VEGF_{165}$, and the growth of ECs, L929 cells, and SMCs are inhibited in late period caused by the delayed and sustained release of PTX. Therefore, the designed drug-carrier/hydrogel system can well meet the clinical requirements of an implant vascular scaffold which requires an encouraged growth of ECs and L929 cells in the early period to reduce the rejection after surgery and an inhibited growth of cells especially SMCs to prevent the vascular intimal hyperplasia.

In the present work, we report a first example, to our best knowledge, of a controllable cell growth scaffold based on

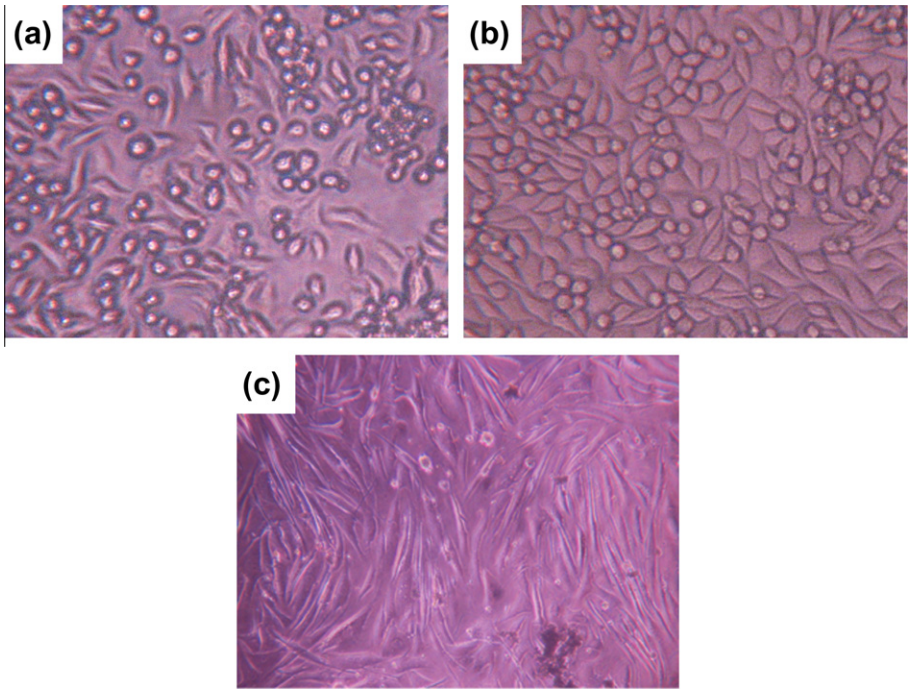

Fig. 7. Optical microscopy photographs of ECs (a), L929 cells (b), and SMCs (c) on the PTX-GPG/$VEGF_{165}$-Alg/PVA composite hydrogel scaffold at day 2 (cultivated with the concentration of 5×10^4 cells/well), with the magnification times of 200. (For interpretation of the references to color in this figure legend, the reader is referred to the web version of this article.)

drug-carrier/hydrogel system. Such controllable cell growth scaffold displays some unique advantages for clinical applications: (1) functional scaffold: the drug-carrier/hydrogel scaffold can encourage the re-endotheliazation in the early days to reduce the rejection after surgery and prevent the vascular intimal hyperplasia in late period; (2) drug delivery for lesion site: the independent release behaviors of drugs from the drug-carrier/hydrogel scaffold can be used for combined drug delivery at lesion site. And the pH-controlled release behavior of both drugs show the targeting effect for drug delivery; (3) convenience: the drug-carrier/hydrogel scaffold is easy to prepare, and the release behavior of each drug can be easily modified by choosing different kinds of drug carriers. We anticipated that this drug-carrier/hydrogel scaffold can be a promising candidate for controlled cell growth in applications of tissue engineering.

4. Conclusions

We prepared a novel hydrogel scaffold for controllable cell growth based on the PTX-GPG/$VEGF_{165}$-Alg/PVA system. The resulting structure of the scaffold is PVA hydrogel network containing PTX-loaded GPG micelles and $VEGF_{165}$-loaded Alg-MPs. $VEGF_{165}$ shows a short-term release, while PTX shows a sustained and long-term release in this hydrogel scaffold. In addition, the in vitro release study shows an interesting phenomenon that the existence of Ca-alginate microparticles (Alg-MPs) in PVA hydrogel can decrease the release rate of PTX due to the reduced hydrogel network pore size when adding Alg-MPs. The viabilities of endothelial cells (ECs) and L929 cells on the PTX-GPG/$VEGF_{165}$-Alg/PVA scaffold shows an encouraged growth in the early period and an inhibited growth in late period. And the viability of smooth muscle cells (SMCs) shows a delayed inhibited growth in late period on the scaffold. The controllable cell growth behavior achieved on the PTX-GPG/$VEGF_{165}$-Alg/PVA hydrogel scaffold is consistent with the requirements of clinical applications of vascular surgery and has the potential for blood vessel tissue engineering applications.

Acknowledgments

This work was supported by National Natural Science Foundation of China (50925308). Supports from projects of Shanghai municipality (09XD1401400, 0952nm05100, 08DZ2230500, and B502) are also appreciated.

Appendix A. Supplementary material

Supplementary data associated with this article can be found, in the online version, at doi:10.1016/j.ejpb.2011.01.015.

References

[1] L. Uebersax, H.P. Merkle, L. Meinel, Insulin-like growth factor I releasing silk fibroin scaffolds induce chondrogenic differentiation of human mesenchymal stem cells, J. Control. Release 127 (2008) 12–21.
[2] Y. Qiu, K. Park, Environment-sensitive hydrogels for drug delivery, Adv. Drug Deliv. Rev. 53 (2001) 321–339.
[3] K.Y. Lee, M.C. Peters, K.W. Anderson, D.J. Mooney, Controlled growth factor release from synthetic extracellular matrices, Nature 408 (2000) 998–1000.
[4] X. Wang, E. Wenk, X. Zhang, L. Meinel, G. Vunjak-Novakovic, D.L. Kaplan, Growth factor gradients via microsphere delivery in biopolymer scaffolds for osteochondral tissue engineering, J. Control. Release 134 (2009) 81–90.
[5] J. Sohier, T.J. Vlugt, N. Cabrol, C. Van Blitterswijk, K. de Groot, J.M. Bezemer, Dual release of proteins from porous polymeric scaffolds, J. Control. Release 111 (2006) 95–106.
[6] X. Shi, Y. Wang, L. Ren, W. Huang, D.A. Wang, A protein/antibiotic releasing poly(lactic-co-glycolic acid)/lecithin scaffold for bone repair applications, Int. J. Pharm. 373 (2009) 85–92.
[7] L. David, V. Dulong, D. Le Cerf, L. Cazin, M. Lamacz, J.P. Vannier, Hyaluronan hydrogel: an appropriate three-dimensional model for evaluation of anticancer drug sensitivity, Acta Biomater. 4 (2008) 256–263.
[8] R.A. Thakur, C.A. Florek, J. Kohn, B.B. Michniak, Electrospun nanofibrous polymeric scaffold with targeted drug release profiles for potential application as wound dressing, Int. J. Pharm. 364 (2008) 87–93.
[9] Y.C. Ho, F.L. Mi, H.W. Sung, P.L. Kuo, Heparin-functionalized chitosan-alginate scaffolds for controlled release of growth factor, Int. J. Pharm. 376 (2009) 69–75.
[10] M.J. Mahoney, K.S. Anseth, Three-dimensional growth and function of neural tissue in degradable polyethylene glycol hydrogels, Biomaterials 27 (2006) 2265–2274.
[11] T.A. Holland, Y. Tabata, A.G. Mikos, Dual growth factor delivery from degradable oligo(poly(ethylene glycol) fumarate) hydrogel scaffolds for cartilage tissue engineering, J. Control. Release 101 (2005) 111–125.
[12] S.A. DeLong, J.J. Moon, J.L. West, Covalently immobilized gradients of bFGF on hydrogel scaffolds for directed cell migration, Biomaterials 26 (2005) 3227–3234.
[13] Y. Luo, M.S. Shoichet, A photolabile hydrogel for guided three-dimensional cell growth and migration, Nat. Mater. 3 (2004) 249–253.
[14] B.K. Mann, A.S. Gobin, A.T. Tsai, R.H. Schmedlen, J.L. West, Smooth muscle cell growth in photopolymerized hydrogels with cell adhesive and proteolytically degradable domains: synthetic ECM analogs for tissue engineering, Biomaterials 22 (2001) 3045–3051.
[15] M.C. Cushing, K.S. Anseth, Materials science. Hydrogel cell cultures, Science (New York, NY) 316 (2007) 1133–1134.
[16] S.M. Willerth, S.E. Sakiyama-Elbert, Approaches to neural tissue engineering using scaffolds for drug delivery, Adv. Drug Deliv. Rev. 59 (2007) 325–338.
[17] T.A. Holland, E.W. Bodde, V.M. Cuijpers, L.S. Baggett, Y. Tabata, A.G. Mikos, J.A. Jansen, Degradable hydrogel scaffolds for in vivo delivery of single and dual growth factors in cartilage repair, Osteoarthritis and cartilage/OARS, Osteoarthr. Res. Soc. 15 (2007) 187–197.
[18] J.O. Winter, S.F. Cogan, J.F. Rizzo 3rd, Neurotrophin-eluting hydrogel coatings for neural stimulating electrodes, J. Biomed. Mater. Res. B 81 (2007) 551–563.
[19] S.J. Taylor, J.W. McDonald 3rd, S.E. Sakiyama-Elbert, Controlled release of neurotrophin-3 from fibrin gels for spinal cord injury, J. Control. Release 98 (2004) 281–294.
[20] N. Gomez, C.E. Schmidt, Nerve growth factor-immobilized polypyrrole: bioactive electrically conducting polymer for enhanced neurite extension, J. Biomed. Mater. Res. A 81 (2007) 135–149.
[21] B.C. Thompson, S.E. Moulton, J. Ding, R. Richardson, A. Cameron, S. O'Leary, G.G. Wallace, G.M. Clark, Optimising the incorporation and release of a neurotrophic factor using conducting polypyrrole, J. Control. Release 116 (2006) 285–294.
[22] D.H. Kim, D.C. Martin, Sustained release of dexamethasone from hydrophilic matrices using PLGA nanoparticles for neural drug delivery, Biomaterials 27 (2006) 3031–3037.
[23] B.I. Rosner, R.A. Siegel, A. Grosberg, R.T. Tranquillo, Rational design of contact guiding, neurotrophic matrices for peripheral nerve regeneration, Ann. Biomed. Eng. 31 (2003) 1383–1401.
[24] Q. Hou, D.Y. Chau, C. Pratoomsoot, P.J. Tighe, H.S. Dua, K.M. Shakesheff, F.R. Rose, In situ gelling hydrogels incorporating microparticles as drug delivery carriers for regenerative medicine, J. Pharm. Sci. 97 (2008) 3972–3980.
[25] K. Moebus, J. Siepmann, R. Bodmeier, Alginate-poloxamer microparticles for controlled drug delivery to mucosal tissue, Eur. J. Pharm. Biopharm. 72 (2009) 42–53.
[26] A. Rosler, G.W. Vandermeulen, H.A. Klok, Advanced drug delivery devices via self-assembly of amphiphilic block copolymers, Adv. Drug Deliv. Rev. 53 (2001) 95–108.
[27] K. Kataoka, A. Harada, Y. Nagasaki, Block copolymer micelles for drug delivery: design, characterization and biological significance, Adv. Drug Deliv. Rev. 47 (2001) 113–131.
[28] P. Satturwar, M.N. Eddine, F. Ravenelle, J.C. Leroux, pH-responsive polymeric micelles of poly(ethylene glycol)-b-poly(alkyl(meth)acrylate-co-methacrylic acid): influence of the copolymer composition on self-assembling properties and release of candesartan cilexetil, Eur. J. Pharm. Biopharm. 65 (2007) 379–387.
[29] S. Ganta, H. Devalapally, A. Shahiwala, M. Amiji, A review of stimuli-responsive nanocarriers for drug and gene delivery, J. Control. Release 126 (2008) 187–204.
[30] E.S. Lee, K. Na, Y.H. Bae, Super pH-sensitive multifunctional polymeric micelle, Nano Lett. 5 (2005) 325–329.
[31] R.M. Sawant, J.P. Hurley, S. Salmaso, A. Kale, E. Tolcheva, T.S. Levchenko, V.P. Torchilin, "SMART" drug delivery systems: double-targeted pH-responsive pharmaceutical nanocarriers, Bioconjug. Chem. 17 (2006) 943–949.
[32] Y. Bae, K. Kataoka, Intelligent polymeric micelles from functional poly(ethylene glycol)-poly(amino acid) block copolymers, Adv. Drug Deliv. Rev. 61 (2009) 768–784.
[33] S.V. Vinogradov, T.K. Bronich, A.V. Kabanov, Nanosized cationic hydrogels for drug delivery: preparation, properties and interactions with cells, Adv. Drug Deliv. Rev. 54 (2002) 135–147.
[34] S.M. Jay, W.M. Saltzman, Controlled delivery of VEGF via modulation of alginate microparticle ionic crosslinking, J. Control. Release 134 (2009) 26–34.
[35] S.T. Lim, G.P. Martin, D.J. Berry, M.B. Brown, Preparation and evaluation of the in vitro drug release properties and mucoadhesion of novel microspheres of hyaluronic acid and chitosan, J. Control. Release 66 (2000) 281–292.

[36] G. Huang, J. Gao, Z. Hu, J.V. St John, B.C. Ponder, D. Moro, Controlled drug release from hydrogel nanoparticle networks, J. Control. Release 94 (2004) 303–311.
[37] R.M. Ramanan, P. Chellamuthu, L. Tang, K.T. Nguyen, Development of a temperature-sensitive composite hydrogel for drug delivery applications, Biotechnol. Prog. 22 (2006) 118–125.
[38] R. Cassano, S. Trombino, R. Muzzalupo, L. Tavano, N. Picci, A novel dextran hydrogel linking trans-ferulic acid for the stabilization and transdermal delivery of vitamin E, Eur. J. Pharm. Biopharm. 72 (2009) 232–238.
[39] M. Goldberg, R. Langer, X. Jia, Nanostructured materials for applications in drug delivery and tissue engineering, J. Biomater. Sci. Polym. Ed. 18 (2007) 241–268.
[40] J.K. Tessmar, A.M. Gopferich, Matrices and scaffolds for protein delivery in tissue engineering, Adv. Drug Deliv. Rev. 59 (2007) 274–291.
[41] F.M. Chen, Y.M. Zhao, H.H. Sun, T. Jin, Q.T. Wang, W. Zhou, Z.F. Wu, Y. Jin, Novel glycidyl methacrylated dextran (Dex-GMA)/gelatin hydrogel scaffolds containing microspheres loaded with bone morphogenetic proteins: formulation and characteristics, J. Control. Release 118 (2007) 65–77.
[42] A. Jaklenec, E. Wan, M.E. Murray, E. Mathiowitz, Novel scaffolds fabricated from protein-loaded microspheres for tissue engineering, Biomaterials 29 (2008) 185–192.
[43] L.E. Freed, F. Guilak, X.E. Guo, M.L. Gray, R. Tranquillo, J.W. Holmes, M. Radisic, M.V. Sefton, D. Kaplan, G. Vunjak-Novakovic, Advanced tools for tissue engineering: scaffolds, bioreactors, and signaling, Tissue Eng. 12 (2006) 3285–3305.
[44] M.W. Laschke, Y. Harder, M. Amon, I. Martin, J. Farhadi, A. Ring, N. Torio-Padron, R. Schramm, M. Rucker, D. Junker, J.M. Haufel, C. Carvalho, M. Heberer, G. Germann, B. Vollmar, M.D. Menger, Angiogenesis in tissue engineering: breathing life into constructed tissue substitutes, Tissue Eng. 12 (2006) 2093–2104.
[45] G.W. Stone, S.G. Ellis, C.D. O'Shaughnessy, S.L. Martin, L. Satler, T. McGarry, M.A. Turco, D.J. Kereiakes, L. Kelley, J.J. Popma, M.E. Russell, Paclitaxel-eluting stents vs. vascular brachytherapy for in-stent restenosis within bare-metal stents: the TAXUS V ISR randomized trial, J. Am. Med. Assoc. 295 (2006) 1253–1263.
[46] N.J. Weissman, S.G. Ellis, E. Grube, K.D. Dawkins, J.D. Greenberg, T. Mann, L.A. Cannon, P.A. Cambier, S. Fernandez, G.S. Mintz, L. Mandinov, J. Koglin, G.W. Stone, Effect of the polymer-based, paclitaxel-eluting TAXUS express stent on vascular tissue responses: a volumetric intravascular ultrasound integrated analysis from the TAXUS IV, V, and VI trials, Eur. Heart. J. 28 (2007) 1574–1582.
[47] K. Pouneh, L. Guy, M. Remi, F. Jeannette, Effect of ionizing radiation on thymidine uptake, differentiation, and VEGFR2 receptor expression in endothelial cells : the role of $VEGF_{165}$, Int. J. Radiat. Oncol. 50 (2001) 213–220.
[48] T. Ostendorf, U. Kunter, F. Eitner, A. Loos, H. Regele, D. Kerjaschki, D.D. Henninger, N. Janjic, J. Floege, $VEGF_{165}$ mediates glomerular endothelial repair, J. Clin. Invest. 104 (1999) 913–923.
[49] H.J. Cho, T.Y. Kim, H.J. Cho, K.W. Park, S.Y. Zhang, J.H. Kim, S.H. Kim, J.Y. Hahn, H.J. Kang, Y.B. Park, H.S. Kim, The effect of stem cell mobilization by granulocyte-colony stimulating factor on neointimal hyperplasia and endothelial healing after vascular injury with bare-metal versus paclitaxel-eluting stents, J. Am. Coll. Cardiol. 48 (2006) 366–374.
[50] X. Wu, L. Huang, Q. Zhou, Y. Song, A. Li, H. Wang, M. Song, Effect of paclitaxel and mesenchymal stem cells seeding on ex vivo vascular endothelial repair and smooth muscle cells growth, J. Cardiovasc. Pharm. 46 (2005) 779–786.
[51] K.Y. Lee, D.J. Mooney, Hydrogels for tissue engineering, Chem. Rev. 101 (2001) 1869–1880.
[52] Y.S. Pan, D.S. Xiong, R.Y. Ma, A study on the friction properties of poly(vinyl alcohol) hydrogel as articular cartilage against titanium alloy, Wear 262 (2007) 1021–1025.
[53] C. Cai, L. Zhang, J. Lin, L. Wang, Self-assembly behavior of pH- and thermosensitive amphiphilic triblock copolymers in solution: experimental studies and self-consistent field theory simulations, J. Phys. Chem. B 112 (2008) 12666–12673.
[54] L. Wei, C. Cai, J. Lin, T. Chen, Dual-drug delivery system based on hydrogel/micelle composites, Biomaterials 30 (2009) 2606–2613.
[55] J. Lin, J. Zhu, T. Chen, S. Lin, C. Cai, L. Zhang, Y. Zhuang, X.S. Wang, Drug releasing behavior of hybrid micelles containing polypeptide triblock copolymer, Biomaterials 30 (2009) 108–117.
[56] D.W. Stepnick, M.K. Peterson, C. Bodgan, J. Davis, J. Wasman, K. Mailer, Effects of tumor necrosis factor α and vascular permeability factor on neovascularization of the rabbit ear flap, Arch. Otolaryngol. Head Neck. Surg. 121 (1995) 667–672.
[57] F. Vogt, A. Stein, G. Rettemeier, N. Krott, R. Hoffmann, J. vom Dahi, A.K. Bosserhoff, W. Michaeli, P. Hanrath, C. Weber, R. Blindt, Long-term assessment of a novel biodegradable paclitaxel-eluting coronary polylactide stent, Eur. Heart J. 25 (2004) 1330–1340.
[58] M. Iza, S. Woerly, C. Danumah, S. Kaliaguine, M. Bousmina, Determination of pore size distribution for mesoporous materials and polymeric gels by means of DSC measurements: thermoporometry, Polymer 41 (2000) 5885–5893.
[59] K. Ishikiriyama, A. Sakamoto, M. Todoki, T. Tayama, K. Tanaka, T. Kobayashi, Pore size distribution measurements of polymer hydrogel membranes for artificial kidneys using differential scanning calorimetry[1], Thermochim. Acta 267 (1995) 169–180.
[60] A. Richter, G. Paschew, S. Klatt, J. Lienig, K.-F. Arndt, H.-J.P. Adler, Review on hydrogel-based pH sensors and microsensors, Sensors 8 (2008) 561–581.
[61] A.L. Ching, C.V. Liew, L.W. Chan, P.W. Heng, Modifying matrix micro-environmental pH to achieve sustained drug release from highly laminating alginate matrices, Eur. J. Pharm. Sci. 33 (2008) 361–370.
[62] I. Freeman, A. Kedem, S. Cohen, The effect of sulfation of alginate hydrogels on the specific binding and controlled release of heparin-binding proteins, Biomaterials 29 (2008) 3260–3268.
[63] A. Wang, C. Tao, Y. Cui, L. Duan, Y. Yang, J. Li, Assembly of environmental sensitive microcapsules of PNIPAAm and alginate acid and their application in drug release, J. Colloid Interface Sci. 332 (2009) 271–279.
[64] Y.N. Dai, P. Li, J.P. Zhang, A.Q. Wang, Q. Wei, Swelling characteristics and drug delivery properties of nifedipine-loaded pH sensitive alginate-chitosan hydrogel beads, J. Biomed. Mater. Res. B 86B (2008) 493–500.
[65] F. Checot, S. Lecommandoux, Y. Gnanou, H.A. Klok, Water-soluble stimuli-responsive vesicles from peptide-based diblock copolymers, Angew. Chem. Int. Ed. Engl. 41 (2002) 1339–1343.
[66] J.E. Chung, M. Yokoyama, T. Okano, Inner core segment design for drug delivery control of thermo-responsive polymeric micelles, J. Control. Release 65 (2000) 93–103.
[67] J. Lin, S. Lin, P. Liu, T. Hiejima, H. Furuya, A. Abe, Phase behavior of ternary systems involving a conformationally variable chain and a randomly coiled polymer, Macromolecules 36 (2003) 6267–6272.
[68] J. Sun, C. Deng, X. Chen, H. Yu, H. Tian, J. Sun, X. Jing, Self-assembly of polypeptide-containing ABC-type triblock copolymers in aqueous solution and its pH dependence, Biomacromolecules 8 (2007) 1013–1017.
[69] N.A. Peppas, S.L. Wright, Drug diffusion and binding in ionizable interpenetrating networks from poly(vinyl alcohol) and poly(acrylic acid), Eur. J. Pharm. Biopharm. 46 (1998) 15–29.
[70] C.S. Brazel, N.A. Peppas, Modeling of drug release from swellable polymers, Eur. J. Pharm. Biopharm. 49 (2000) 47–58.
[71] C.L. Grosskreutz, B. Anand-Apte, C. Duplaa, T.P. Quinn, B.I. Terman, B. Zetter, P.A. D'Amore, Vascular endothelial growth factor-induced migration of vascular smooth muscle cells in vitro, Microvasc. Res. 58 (1999) 128–136.
[72] M. Inoue, H. Itoh, M. Ueda, T. Naruko, A. Kojima, R. Komatsu, K. Doi, Y. Ogawa, N. Tamura, K. Takaya, T. Igaki, J. Yamashita, T.H. Chun, K. Masatsugu, A.E. Becker, K. Nakao, Vascular endothelial growth factor (VEGF) expression in human coronary atherosclerotic lesions: possible pathophysiological significance of VEGF in progression of atherosclerosis, Circulation 98 (1998) 2108–2116.